

Fermi National Accelerator Laboratory

FERMILAB-Conf-98/070

Friction Model of the 2.5mts SDSS Telescope

Claudio H. Rivetta and Sten Hansen

*Fermi National Accelerator Laboratory
P.O. Box 500, Batavia, Illinois 60510*

February 1998

Published Proceedings of the *Spie International Symposium on Astronomical Telescopes and Instrumentation*, Hawaii, March 20-27, 1998

Operated by Universities Research Association Inc. under Contract No. DE-AC02-76CH03000 with the United States Department of Energy

Disclaimer

This report was prepared as an account of work sponsored by an agency of the United States Government. Neither the United States Government nor any agency thereof, nor any of their employees, makes any warranty, expressed or implied, or assumes any legal liability or responsibility for the accuracy, completeness, or usefulness of any information, apparatus, product, or process disclosed, or represents that its use would not infringe privately owned rights. Reference herein to any specific commercial product, process, or service by trade name, trademark, manufacturer, or otherwise, does not necessarily constitute or imply its endorsement, recommendation, or favoring by the United States Government or any agency thereof. The views and opinions of authors expressed herein do not necessarily state or reflect those of the United States Government or any agency thereof.

Distribution

Approved for public release; further dissemination unlimited.

Friction model of the 2.5mts SDSS telescope

Claudio H. Rivetta, and Sten Hansen

Fermi National Accelerator Laboratory
P.O Box 500, Batavia IL 60510 ,USA.

ABSTRACT

The 2.5mts telescope designed for the Sloan Digital Sky Survey (SDSS) is a mechanical structure that presents five degree-of-freedom. Azimuth, altitude and the instrument rotator axis are fitted with servo controls. The low frequency dynamic are dominated by the bearing friction. Several mathematical models have been presented in the literature to include its effect into the dynamic model of mechanical structures. The model employed in this paper includes consideration of the Striebeck effect, dynamic behavior at very low velocities and the pre-sliding at near zero-velocity. Results of the parameter estimation of the friction model of the three principal axes are presented as well as the behavior of the structure when different torque stimuli are applied.

The mathematical model used to include the friction phenomena into the telescope dynamic model is simple. It does a good job of describing the friction over a wide range of velocities but particularly at or below siderial rate. It is a straight forward process to determine the parameters and, in simulations, does not require large amounts of computer time.

Keywords: *Friction model, Friction parameter estimation, System modeling*

1. INTRODUCTION

The 2.5 mts SDSS Telescope is designed to accurately track the sky for long periods at low speed during drift scanning, then to slew rapidly to a different region in the sky before beginning a new scan. The mechanical structure of the telescope is relatively light and stiff, has many resonances at frequencies above 10Hz. The telescope has five degrees of freedom (DOF) as opposed to as many as eight DOF on some telescopes. The need to do drift scanning precludes the use of tilt/tip control on the secondary mirror and there is no controllable adjustment of the primary to secondary distance. Control is performed on the azimuth, altitude and instrument rotator axes. The two remaining degrees of freedom associated with tilt about the telescope base are restricted by pre-loaded springs acting on four capstans rolling on the perimeter of the azimuth drive disk. All the drive motors are permanent magnet DC motors driven in current mode by linear power amplifiers. The motion from these motors is transmitted to the axes by friction between the capstans and their respective axis drive disks. The motors are located on opposite sides of the azimuth drive disk, two motors drive two altitude axis disks, and a single motor with a harmonic reducer drives the rotator disk.

In this system, friction is one of the important perturbations to consider in the design of the servo controller. The perturbations can induce oscillations either while moving at low speeds or while holding stationary if the controller is designed without considering the friction effects present during these modes of operation. At each axis, the friction effect is the combination of the individual bearing friction. The model described considers the overall effect of bearings at each axis. In figure 1, the major contribution to friction are shown :

1. Azimuth- 1-a) Lower azimuth bearing , 1-b) Upper azimuth bearings (capstans)
2. Altitude- 2-a) Altitude bearing , 2-b) Capstans
3. Instrument rotator- 3-a) Central bearing, 3-b) Harmonic Drive.

Technical information about those bearings can be found in a SDSS report[1].

¹ Further author information - C.H.R. (correspondence): E-mail:rivetta@fnal.gov; Telephone (630)-840-8035

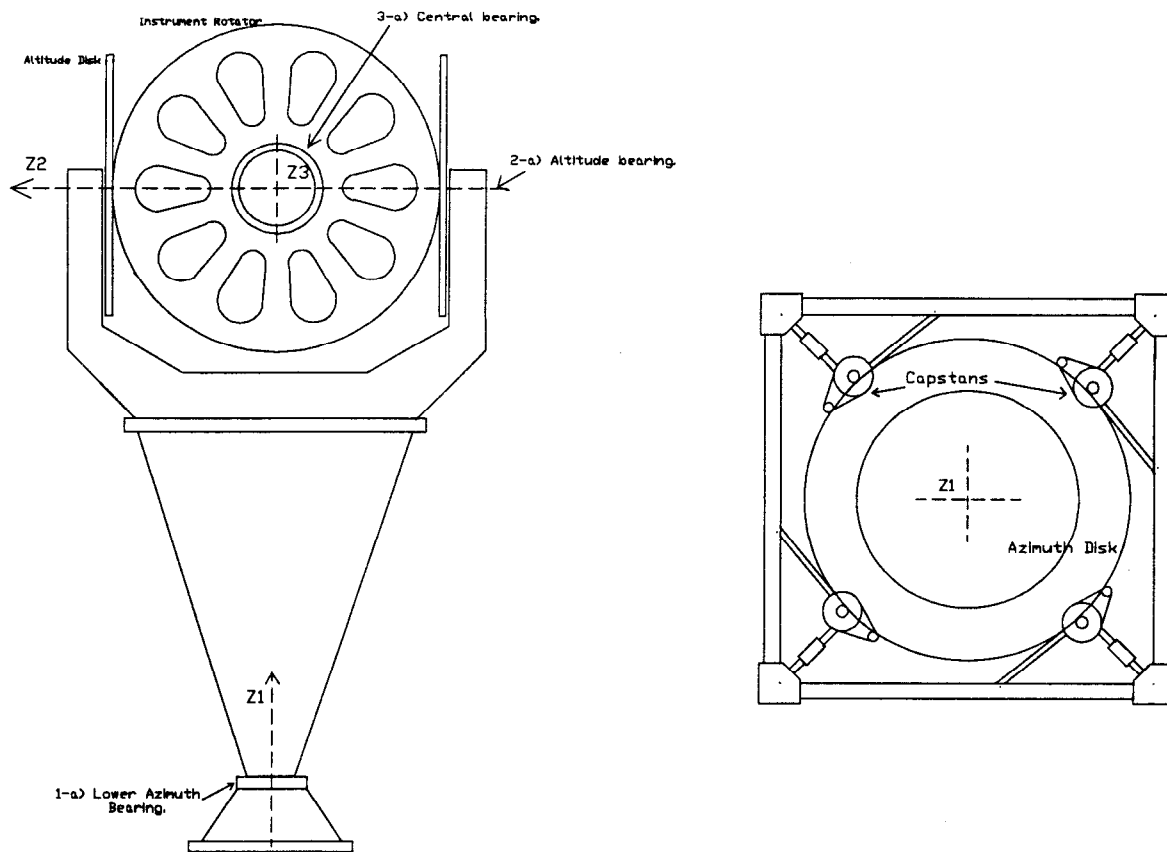


Figure 1.- Left: View of telescope pointing at horizon. Right: Top view of Azimuth disk.

Friction is usually modeled as a static map between velocity and friction force or torque. It includes static, Coulomb and viscous friction components. However, there are several interesting properties observed in systems with friction that do not respond instantaneously to a change of velocity. Examples of these includes: stick-slip motions, pre-sliding displacement, Dahl effect and frictional lag. Several models have been presented in the literature to capture dynamic behavior of the friction [2] [3] [4]. In general, they are non linear parametric models and their successful application depends very much on the quality of the estimated parameters. In this paper, a model with six parameters is used to describe friction behavior of the three principal axes of the telescope. Estimation of these parameters is based on data collected in two sets of measurements. First the static parameters are estimated from data collected during operation at constant velocity. Then dynamic parameters are derived using non linear optimization methods.

The paper is organized as follows. Section 2.1 presents a short description of the dynamic model of the telescope since it is necessary to estimate the dynamic friction parameters. Section 2.2 gives a qualitative description of the friction phenomena and mathematically formulates the friction model used in this analysis. Section 3 presents the two step method for estimating the friction parameters and shows the results of measurements and simulations using the friction model with the estimated parameters.

2. FRICTION MODEL ANALYSIS

2.1 Dynamic model of telescope

Since the control is performed only on three axes, the analysis is performed considering the telescope as a 3 DOF structure. To estimate the friction model parameters, each axis is driven at low velocity and a rigid model is used to mathematically describe the dynamic behavior of the telescope. The model can be written as:

$$M(\theta) \cdot \frac{d^2\theta}{dt^2} + V(\theta, \frac{d\theta}{dt}) + G(\theta) + T_{friction} + T_{disturbances} = T \quad (1)$$

where:

$\theta = [\theta_1 \ \theta_2 \ \theta_3]^T$: Position of reference axis of joints 1,2 and 3. (3x1 vector), ([..]^T denotes transpose)

$T = [T_1 \ T_2 \ T_3]^T$: Mechanical torque applied to the structure by the capstans. (3x1 vector)

$M(\theta)$: Mass matrix. (3x3 matrix)

$G(\theta)=[G_1 \ G_2 \ G_3]^T$: Gravity vector (3x1 vector)

$V(\theta, \frac{d\theta}{dt})$: Centrifugal and Coriolis vector. (3x1 vector)

$T_{friction}$: Friction torque on joints 1,2 and 3.

$T_{disturbances}$: Disturbance torque (wind disturbance, etc.) (3x1 vector)

The parameters or elements of the matrices $M(\theta)$, $C(\theta)$, $B(\theta)$ and $G(\theta)$ can be derived mathematically using solid model analysis. Entries of $G(\theta)$ are equal to zero if the corresponding link is in balance. In equation 1, $T_{disturbances}$ is neglected due to the fact measurements were performed inside a building and wind disturbances is negligible. $T_{disturbances}$ can consider secondary effects as torque ripple, coupled vibrations, etc., that are part of the noise term present in the data.

Torques T_1 and T_2 corresponding to azimuth and altitude axis are generated by DC motors driven in current mode and coupled directly to the structure by friction capstans. Because of the very low drive ratios (25:1), the torsional rigidity of the capstan is very high, and mathematically the torque can be expressed as:

$$T_i = 2 \cdot n_c \cdot K_T \cdot i_{ref} \quad i = 1, 2 \quad (2)$$

where:

n_c = ratio between the capstan diameter and azimuth/altitude disc diameter.

K_t = Torque constant.

i_{ref} = Motor current.

the factor 2 takes into account each axis is driven by two motors.

The instrument rotator is driven by a harmonic drive reducer and a DC motor. The output of this actuator then transmits the torque to the instrument rotator disk through a friction capstan. The harmonic drive gearing has significant elasticity and has to be taken into account in the model of the driver. Using as reference frame that of the rotator disk and assuming a simplified model for the DC motor can be used because it is driven in current mode, the rotator driver can be modeled by the following equations:

$$T_m = n_c \cdot K_T \cdot i$$

$$T_3 = (n_c)^2 \cdot K \cdot (\theta_s - \theta_3) \quad (3)$$

$$\frac{d^2 \theta_s}{dt^2} \cdot J_m \cdot (n \cdot n_c)^2 = T_m - T_3 - n_c \cdot T_{fHD}$$

where:

K_T : DC motor torque constant

T_m : Motor torque

J_m : Moment of inertia of motor and tachometer

T_{fHD} : Harmonic drive friction

T_m : Motor torque

n : Harmonic drive gear ratio.

n_c : Diameter ratio between capstan and rotator

K : Spring rate of harmonic drive

T_3 : Torque applied to the instrument rotator.

θ_s : Position of motor shaft reflected on instrument rotator frame

θ_3 : Position of instrument rotator axis

The harmonic drive compliance not constant. It increases as the torque developed by the actuator increases. This effect can be introduced into the model by defining a spring rate function $K(T_3)$. The harmonic drive also introduces hysteresis which is not included in this relatively simple model [5] [6].

2.2 Friction Model

A good friction model is necessary to analyze stability, predict limit cycles, find controller gains, perform simulations, etc. Most of friction models use the classical approach that defines static, Coulomb and viscous friction. In applications with high precision positioning and with low velocity tracking, these models perform poorly. A better description of the friction phenomena for low speeds and especially when crossing zero velocity is required. Friction is a natural phenomenon that is quite hard to model and it is still not completely understood. In the face of these difficulties, a usable model must nevertheless still be able to account for the majority of observed friction phenomena. By analyzing friction as a function of velocity is possible to separate the problem into four dynamic regimes: static friction, boundary lubrication, partial fluid lubrication and full fluid lubrication as is depicted in figure 2.

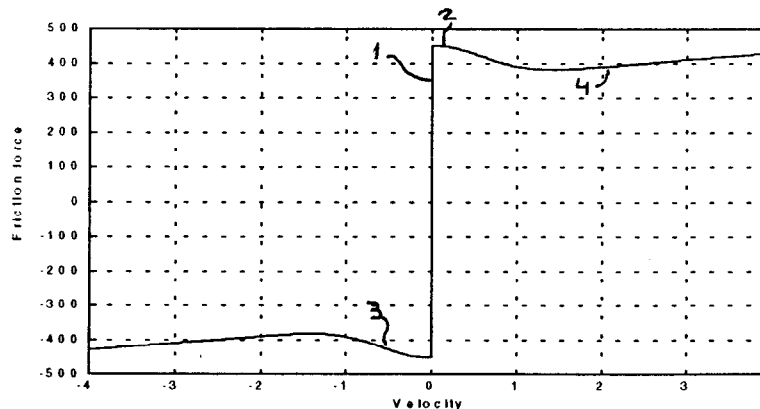


Figure 2,- Static Friction - Velocity curve. 1-No Sliding; 2-Boundary Lubrication; 3- Partial Fluid Lubrication; 4- Full Fluid Lubrication

In the static friction regime, the contact between surfaces occurs at asperity junctions and display two important behaviors. The material at the contact points deforms elastically, giving rise to *presliding displacement*. Both the boundary film of the bearing lubricant and the asperity junctions deform plastically, giving rise to *rising static friction*. It is often assumed when studying friction that there is no motion while in static friction, but it is know that contacts points are compliant in both the normal and tangential directions. Experimental observations show that a junction in static friction regime behaves like a spring. There is a displacement which is proportional to the applied force, up to a critical force, at which breakaway occurs. The tangential stiffness of asperity is a function of asperity geometry, material elasticity and applied normal force. When the normal force is changing, the behavior may be quite complex because normal force, normal stiffness and tangential stiffness are all nonlinear, interacting functions of normal displacement. As a first approximation, it is possible to assume the tangential force developed due to displacement is proportional to the displacement away from the equilibrium position. In the particular case of the SDSS telescope, we observe elastic behavior over a displacement range of the order of a few arc seconds.

In the second regime, at very low sliding, fluid lubrication is not very important because the velocity is not adequate to build a fluid film between the surfaces. The contact is solid-to-solid and there is shearing. Due to boundary lubrication is a process of shear in a solid is assumed the friction is higher than for fluid lubrication. As the velocity increases, lubricant is drawn into the contact zone. Lubricant is brought in this region thought motion, either by sliding or rolling. It constitutes the third regime denominated partial lubrication. There is a gradual transition from solid-to-solid contact to film sliding, giving rise to the typical Stribeck effect. In that, the friction goes down as the velocity increases. This is the most difficult phenomena to model. From the control point of view, it is important to understand in addition the dynamics of partial fluid lubrication with changing velocity. The studies show a time lag between the change in the velocity or load conditions and the change in friction to its new steady state level. This time or phase lag is called frictional memory.

As the velocity increases, the solid-to-solid contact is eliminated and the sliding parts are separated by fluid lubricant. It constitutes the last part of the Stribeck effect and is called full fluid lubrication. From this point, the friction is well modeled by the Coulomb and viscous friction.

A mathematical model describing the friction has to include all the friction regimes and the dynamic behavior found at pre-sliding and at low velocities (frictional memory). One possible technique for describing frictional memory in the model was to consider a pure time-lag as part of the static friction characteristic [7]. An alternative method is to use state variable models. The state variable model incorporates a dependence on displacement history. A typical model posses the following three properties for constant normal stress:

- .) a steady-state dependence on velocity;
- .) an instantaneous dependence on velocity; and
- .) an evolutionary dependence on characteristic sliding distances.

The steady-state effect represents what is generally called the static curve, the instantaneous effect means that an instantaneous change in velocity results in an instantaneous change in the same direction of the friction force developed. The third point indicates that following a sudden change in velocity, the steady-state friction force is reached asymptotically by an exponential decay.

In general, the model for n state variables can mathematically be given by:

$$F_f(t) = f(v, z_1, z_2, \dots, z_n) \tag{4}$$

$$z_i = g_i(v, z_1, z_2, \dots, z_n), \quad i = 1, 2, \dots, n$$

This form implies a sudden change in velocity v cannot produce a sudden change in the states z_i , but affects its time derivative. Physical interpretations of the state variables are possible [1] [8]. A first order model that includes the Striebeck effect was presented by Canudas de Wit *et. al*. It is a modification of the Dahl model and the internal state has physical

interpretation: it describes the average deformation of microscopic bristles and is the model used in this analysis. It can be derived assuming surfaces in contact are irregular at a microscopic level and they make contact at a number of asperity or bristles. When a tangential force is applied, these bristles deflect as springs giving rise to the friction force. If the force is large enough some bristles deflect so much that they will slip. The process is highly random due to the irregular form of surfaces. The model assumes the internal state is the average deflection of bristles, denoted as z . Mathematically it is related to the velocity by:

$$\frac{dz}{dt} = v - \frac{|v|}{g(v)} \cdot z \quad (5)$$

where v is the relative velocity between the two surfaces. The first term points the deflection is proportional to the integral of the relative velocity. The second is included to make the deflection converge to the value

$$z_{ss} = g(v) \cdot \text{sgn}(v) \quad (6)$$

under steady state conditions ($v = \text{constant}$). The force generated from bending the bristles can be added to the one that take into account the viscous friction giving ;

$$F_f(t) = \sigma_0 \cdot z + \sigma_1 \cdot \frac{dz}{dt} + \sigma_2 \cdot v \quad (7)$$

where σ_0 is the stiffness, σ_1 a damping coefficient and σ_2 is the viscous coefficient. In the steady state (constant velocity), the friction force is described as

$$F_{fss}(v) = \sigma_0 \cdot g(v) \cdot \text{sgn}(v) + \sigma_2 \cdot v \quad (8)$$

Several approximations for the $\sigma_0 \cdot g(v)$ function have been proposed to model the steady-state friction-velocity mapping [3] [9]. The more significant are:

$$F_{fss}(v) = [Fc + \frac{(Fs - Fc)}{1 + (\frac{v}{vs})^2}] \cdot \text{sgn}(v) + \sigma_2 \cdot v \quad (a)$$

$$F_{fss}(v) = [Fc + (Fs - Fc) \cdot e^{-(v/vs)^2}] \cdot \text{sgn}(v) + \sigma_2 \cdot v \quad (b)$$

where F_s is the level of static friction, F_c is the Coulomb friction and v_s is an empirical parameter. In other approximations, the square power in 9b is substituted with a parameter that ranges from $1/2$ to 2. The four parameters in equation 9 can be estimated based on the friction-velocity curve determined experimentally. In addition, the model enables one to define two sets of parameters if the friction-velocity curve is direction dependent.

Dynamically the model shows at velocity $v \cong 0$ *presliding displacement* but not *rising static friction*. This feature can be included in equation 9 if one considers the parameter F_s as function of the dwell time [9]. It is not included in our formulation, due to the fact that this part of the model is important mainly for determining the amplitude of stick-slip oscillations. The additional parameters σ_0 and σ_1 in equation (7) are estimated based on data collected when telescope was driven by a time dependent torque.

3. Friction parameter estimation

Considering both the friction model described above and the dynamic model of the telescope it is possible to determine the six parameters that characterize the friction model. Parameters corresponding to the dynamic telescope model

were calculated using solid model analysis. Since each axis of the telescope is rotational, the friction is characterized by a friction torque instead of a force and the velocity is angular (ω). The total contribution to the friction torque at each axis is the sum of the individual friction contribution of all the mechanisms involved. The model is based on the total friction and no partial or individual study has been performed. Two sets of measurement have been performed: static or friction-velocity curve determination and dynamic, in which the system is driven by a time dependent torque while velocity or position is recorded. The data collected under real operating conditions have higher dispersion than those of research reports whose data is collected under much more controlled conditions.

3.1 Azimuth

For azimuth two sets of measurements were recorded. The axis was driven at constant velocity by a closed-loop feedback using two motors connected in serie. Altitude and instrument rotator are held in position. The friction-velocity data was obtained by averaging the measured velocity and the motor current at different speeds and moving the structure both clockwise and counter clockwise. These points are used to estimate the four parameters in equation (9-b). The goal was to collect good data at low velocity in order to improve the accuracy of the model at tracking speeds. A nonlinear optimization algorithm is used to fit the data to the equation (9-b)[10]. The cost function to be minimized is:

$$\min_{\sigma_2, v_s, T_s, T_c} \sum_{i=1}^n [T_{fss}(\omega_i) - \hat{T}_{fss}(\omega_i)]^2 \quad (10)$$

where $\hat{T}_{fss}(\omega)$ is the estimated torque (equation 9b) and $T_{fss}(\omega)$ is the torque measured at constant velocity ω . The optimization routine ran independently for positive and negative velocities. Results of the experimental and the estimated friction-velocity map are shown in figure 3.

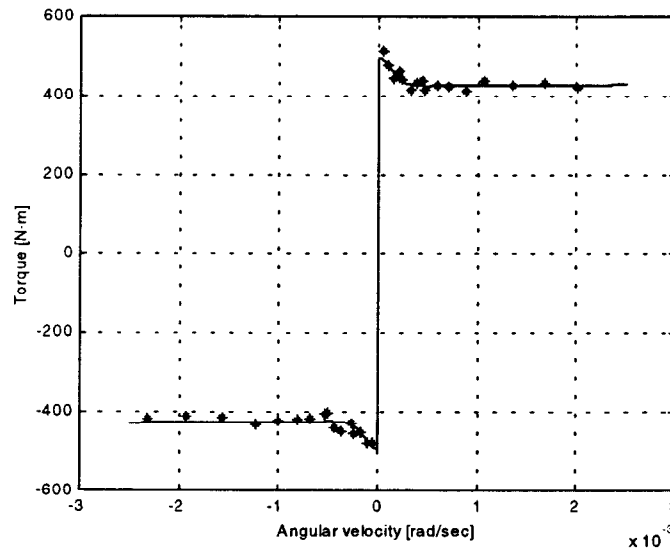


Figure 3.- Azimuth axis. Static friction-velocity curve.
(*) Experimental Data, (—) Model.

Another set of measurements was obtained driving, in open loop, the azimuth axis with a time dependent torque. This test was performed using both sine wave and a triangular wave of different amplitudes. For the best estimation of σ and σ_1 it is desirable to keep the peak torque below that of the breaking friction value. The frequency of the driving signal was relatively low and the dynamic model for azimuth axis can be reduced to:

$$T_1 = J_{z1} \frac{d\omega_1}{dt} + Tf \quad (11)$$

where J_{zz1} is the moment of inertia of the telescope about the rotation axis Z_1 , the friction torque T_f is given by equation (7) and T_l is the motor torque. The recorded is used to search for a set of parameters σ_0 and σ_1 that minimize the following output error cost function [10]:

$$\min_{\sigma_0, \sigma_1} \sum_{i=1}^n (\omega_i - \hat{\omega}_i)^2 \quad (12)$$

where ω_i is the i -th sampled system velocity and $\hat{\omega}_i$ is the i -th value of the model output velocity obtained by solving equations (5), (7) and (11). Equations (5) and (7) use the parameters estimated before. To set suitable initial guess for σ_0 and σ_1 is possible to use some of the data collected. In particular, when the azimuth is driven with a torque following a triangle wave with amplitude lower than the breaking friction it is possible to estimate the initial values of the parameters. Using the initial guess, the parameters can be optimized by a numerical method in which the optimization algorithm calls a Runge-Kutta routine to compute $\hat{\omega}_i$, using (5), (7) and (11). Figure 4 shows the results of the measurements and those obtained using the model with the estimated parameters.

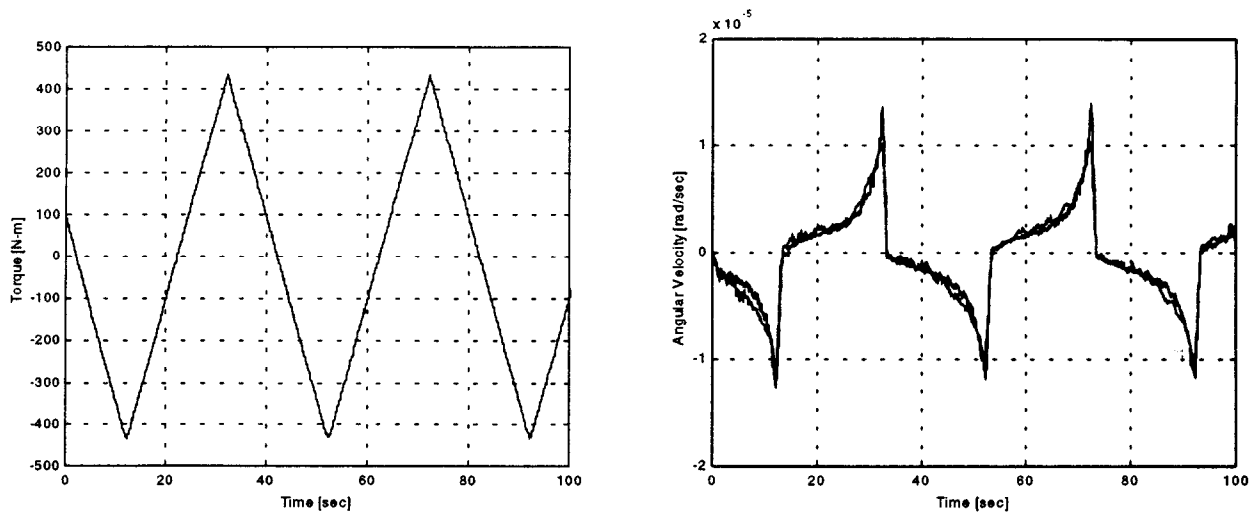


Figure 4.a- Left: Input Torque; Right: Output velocity (Experimental and Model Response).

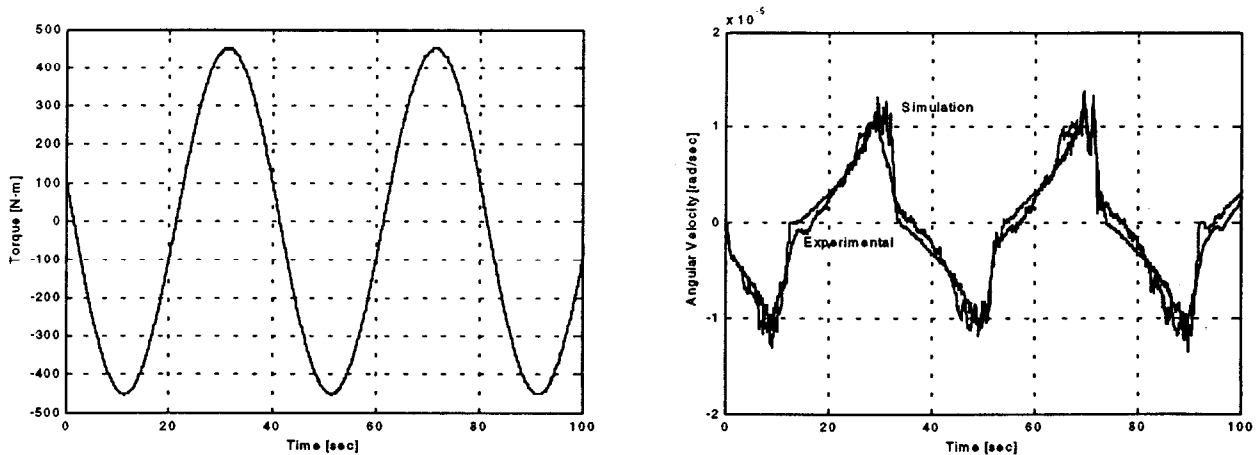


Figure 4.b- Left: Input Torque; Right: Output velocity (Experimental and Model Response).

Figure 4a and 4b show both the experimental and simulated results when the input torque is lower than the breaking friction. On the scale shown, it is very difficult to distinguish the two traces from each other. Figure 4c depicts the response when the input torque is slightly higher than the breaking friction.

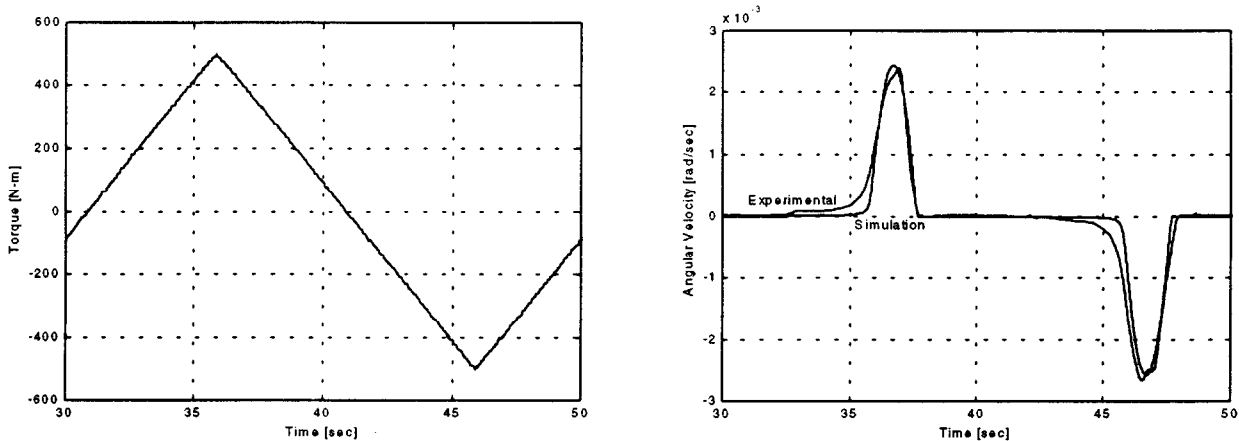


Figure 4.c- Left: Input Torque; Right: Output velocity (Experimental and Model Response)

Further improvement in the results are necessary due to fact that the measurements were taken with the telescope only partially assembled. When the secondary support trust, primary and secondary mirrors and instruments are in place, the expectation is that the values of friction parameters will rise due to the increase of normal force on central bearing.

3.2 Altitude

As stated before, the telescope was partially assembled at the time the data was collected. The altitude link, without the secondary trust and the primary and secondary mirrors is out of balance. To model this situation, $G(\theta)$ in equation (1) is not zero. In this case, the estimation of the static curve parameters is complicated by this term. The dynamic model for altitude axis can be reduced to:

$$T_2 = J_{zz2} \cdot \frac{d\omega_2}{dt} + T_f + G_2(\theta) \quad (13)$$

where:

J_{zz2} : Moment of inertia of the altitude structure about the rotation axis Z_2 .

T_f : Friction torque given by equation (7).

T_2 : Motor torque.

$G_2(\theta) \cong m_2 \cdot g \cdot X_2 \cdot \theta$ for small rotational angles.

m_2 : Mass of altitude and instrument rotator structure.

g : Gravity acceleration

X_2 : Distance between the altitude rotation axis and center of mass of altitude and instrument rotator structure.

The estimation of all the six parameters was based on data collected when the altitude axis was driven in open loop by a time dependent torque. The driving signals were, again, a sine wave and a triangle wave with different amplitudes. First the dynamic parameters were estimated using the data collected when the altitude structure is driven by a triangular wave torque with amplitude lower than the breaking friction. Then the static parameters are estimated using the data recorded when the input torque was higher than the static friction. Figure 6a shows the experimental results and those obtained using the friction model when the input torque amplitude is lower than the breaking friction.

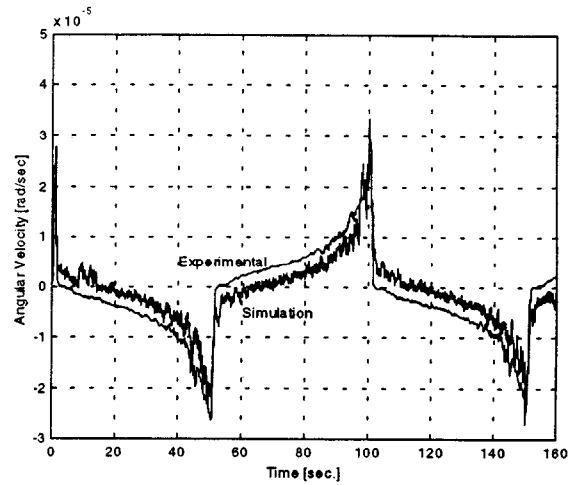
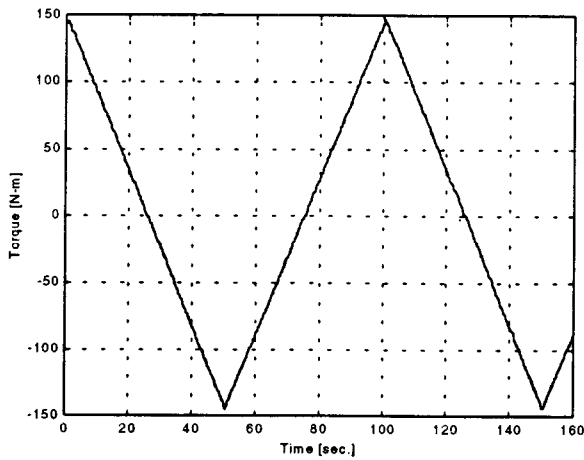


Figure 6a.- Left: Input Torque; Right: Output velocity (Experimental and Model Response).

Figure 6b shows the case when the input torque is slightly higher than the breaking friction torque. The velocity measured is superposed with the data obtained by simulation using the estimated parameters. On the scale shown, it is difficult to distinguish the traces from each other. Figure 7 depicts the computed static friction curve using the friction model with the estimated parameters.

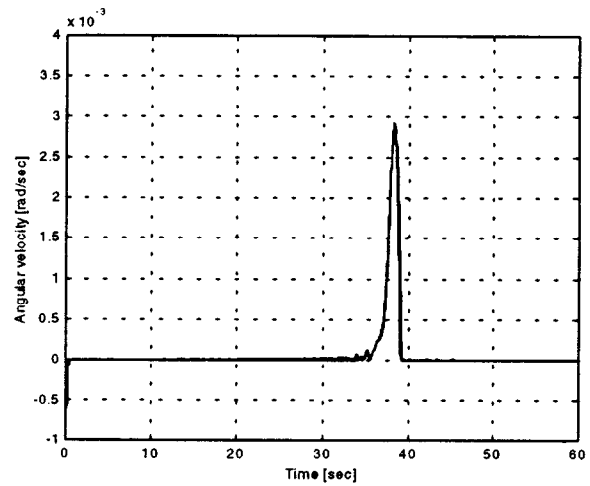
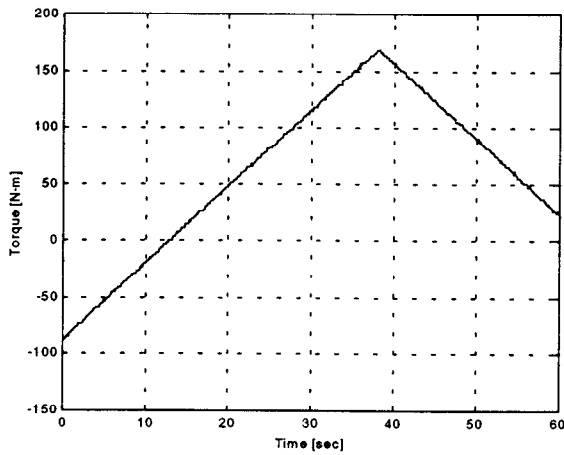


Figure 6b.- Left: Input Torque; Right: Output velocity (Experimental and Model Response).

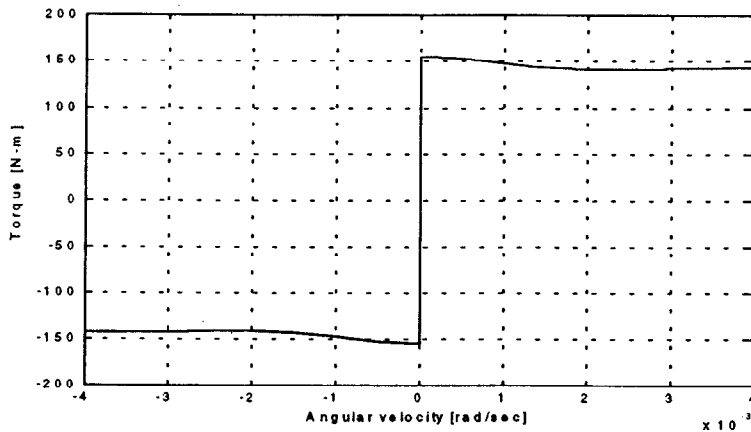


Figure 7.- Altitude axis. Static friction-velocity curve.

3.3 Instrument rotator

A procedure similar to that on azimuth axis was follow to estimate the static friction parameters at instrument rotator axis. At constant velocity, from equations (1) and (3) the motor torque is:

$$T_3 = T_f + n_c \cdot T_{fHD} \quad (13)$$

For this case, the friction -velocity map must include both the friction at the rotator central bearing and at the harmonic drive. The harmonic drive friction in equation (13) is not negligible. Figure 8 depicts the experimental data and the static curve using the estimated parameters. Based in the model of the harmonic drive (eq. 3), the rotator bearing friction T_f and the harmonic drive friction T_{fHD} act at both sides of the coupling spring. In that case, further refinement in the measurements it is necessary to separate the effect of each friction torque. It affects the estimation of the dynamic parameters of the friction. For this case, it will be necessary to identify the friction parameters of the harmonic drive and then proceed indirectly with the friction parameters of the central bearing.

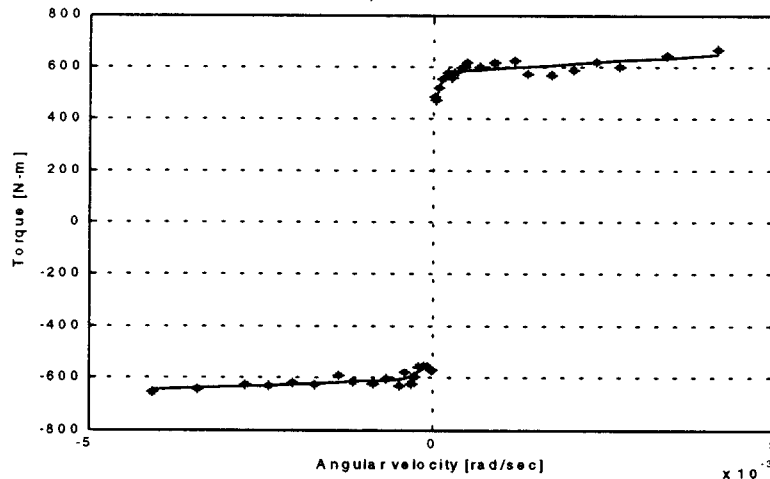


Figure 8.- Instrument rotator axis. Static friction-velocity curve.
(*) Experimental Data, (—) Model

The estimated parameters constitute a first attempt in the characterization of the telescope friction. They are dependent on the normal force applied on each bearing and these forces will change when the telescope is completely assembled. During operation, the normal force on each bearing can be considered constant, except at the rotator bearing with its cantilevered instrument load. It is assumed, however that the very large initial pre-load of that bearing is much higher than the normal force variation when the altitude axis changes in position. In that case, the effect on friction parameters should be negligible. This analysis does not include parameter variation with the temperature and aging.

4. CONCLUSIONS

The model of the friction torque used in this analysis describes the friction over a wide range of velocities with good accuracy. Two different sets of experiments were used to estimate the static and dynamic friction parameters. A non-linear optimization technique was used for computing them. The friction model clearly shows two different behaviors of the telescope. One when the velocity is high and the friction is due to the Coulomb effect and viscosity. In this regime, it is possible to analyze the performance of the telescope using a linear model around the operation point. A different behavior is observed when the velocity is near to zero. The dynamics are more complicated and the stability and performance depend on the parameters σ_0 and σ_1 of the friction model. The controller to be designed has to exhibit stable operation in both cases and furthermore must reject perturbations at a specified level.

5. ACKNOWLEDGEMENTS

This work was performed at Fermi National Accelerator Laboratory which is operated by Universities Research Association, Inc. under contract with the U. S. Dept. of Energy.

The authors wish to thank the Apache Point Observatory staff, in particular Jon Davis, and the SDSS collaboration for the cooperation and assistance during the data collection.

6. REFERENCES

1. W. Siegmund, and C. Hull, "2.5-m Telescope drive measurements IV: Acceptance testing", *SDSS Telescope Technical Note # 19950608_01*, <http://www.apo.nmsu.edu/Telescopes/SDSS/eng.papers>. March 1997.
2. C. Canudas de Wit, H. Olsson, K.J.Astron, and P. Lischinsky, "A new model for control of systems with friction", *IEEE Trans. Automatic Control*. **TAC-40, No.3**, pp.419-425, March 1995.
3. B.Armstrong-Helouvry, P. Dupont, and C. Canudas de Wit, "A survey of models, analysis tools and compensation methods for the control of machines with friction", *Automatica*, **Vol.30, No.7**, pp.1083-1138, 1994.
4. D. Haessing, Jr., and B. Friedland, "On the modeling and simulation of friction", *SPIE Acquisition, Tracking and Pointing V*, **Vol.1483**, pp.383-396, 1991.
5. T.Tuttle, and W. Seering, "Modeling a Harmonic Drive Gear Transmission" *IEEE International Conference on Robotics and Automation*. ISN 1050-4729/93, pp.624-629., 1993.
6. W. Seyfferth, A.J. Maghzal, J.Angelos, "Nonlinear modeling and parameter identification of HD robotic transmissions", *IEEE International Conference on Robotics and Automation*. ISN 0-7803-1965-6/95, pp.3027-3032., 1995
7. D. Hess, and A. Soom, "Friction at a lubricated line contact operating at oscillating sliding velocities. *Journal of Tribology*, **112 (1)** pp. 147-152, 1990.
8. P. Dupont, and E. Dunlop, "Friction modeling and control in boundary lubrication", *Proc 1993 American Control Conferences*, pp. 1910-1914, San Francisco - CA, June 1993.
9. B.Armstrong-Helouvry, "Stick-Slip and control in low-speed motion", *IEEE Trans. Automatic Control*. **TAC-38, No.10**, pp.1483-1496, October 1993.
10. C. Canudas de Wit, and P. Lischinsky, "Adaptive friction compensation with partially known dynamic friction model", *International Journal of Adaptive Control and Signal Processing - Special issue on adaptive systems with nonsmooth nonlinearities (to be published)*